

The Impact of Optical Fiber Type on the Temperature Measurements in Distributed Optical Fiber Sensor Systems

Mateusz Łakomski, Mateusz Plona, Bartłomiej Guzowski

Department of Semiconductor and Optoelectronic Devices, Lodz University of Technology, Politechniki Ave. 10, 93-590 Lodz, Poland

Iyad S. M. Shatarah

Institute of Electronics, Lodz University of Technology, Politechniki Ave. 10, 93-590 Lodz, Poland

Abstract: This paper presents the capabilities of using distributed optical fiber sensors to obtain the temperature profile of an optical path made of silica telecom optical fiber. The impact of the optical fiber type on the temperature measurements is also observed. Two types of optical fibers are tested: standard G.652.D and low-loss G.654.C. DOFS systems for temperature measurements are based on the phenomenon of Raman or Brillouin backscattering. In case of Brillouin-based systems, the spectral properties depend on the type of optical fiber and its parameters. The Brillouin frequency shift depends on the temperature around the fiber, as well as the strain applied to the optical fiber. The presented results show that temperature coefficient can also vary depending on the optical fiber type. For the standard G.652.D optical fiber, the temperature coefficient equals 1.12 MHz/°C and 1.14 MHz/°C depending on the tracked peaks, while for the low-loss G.654.C fiber it equal 1.4 MHz/°C.

Keywords: optical fiber, DOFS, OTDR, Brillouin scattering

1. Introduction

Depending on the amount of sensing points, optical fiber sensors can be defined as single-point, multi-point or distributed sensors. Optical fiber sensors can be classified, based on the principle of operation, into [1]:

- intensity-modulated, which rely on the measurement of attenuation along the optical fiber, e.g.: micro- and macro-bend sensors, evanescent wave sensors,
- phase-modulated, which measure the interference of the optical fibers based on the interferometry principle, e.g.: Mach-Zehnder, Michelson, Sagnac and Fabry-Perot interferometers,
- wavelength-modulated, which rely on the measurement of wavelength variations, e.g.: Fiber Bragg Grating, fluorescence sensors,
- polarization-based, which implement the birefringence phenomenon in order to determine the change in the refractive

index resulting from the change in polarization, e.g.: rotator Faraday rotating sensor,

- scattering-based, which implement the light scattering phenomenon in order to measure physical quantities variations in the optical fiber environment, such as electromagnetic fields, temperature and strain, e.g.: Rayleigh, Brillouin and Raman reflectometry.

Distributed optical fiber sensors (DOFS) have been popular in the past years due to the growing need to perform measurements at long distances with a respectful spatial and measurement resolutions, as well as the relatively simple and low-cost construction of the sensing system [2]. One optical fiber can replace a huge number of discrete sensors, covering distances up to tens of kilometers, providing thousands of measurement points depending on the system spatial resolution [3]. Thanks to the huge development in optical fibers, their immunity to electromagnetic interferences and durability [4, 5], DOFS systems can easily outperform conventional sensing systems, not only by the means of measurements quality, but also by the wide spectrum of applications [6–8] that can utilize these systems, even in the harsh environments [9].

The studies of the backscattered bands: Rayleigh, Brillouin and Raman, proved their dependency on the physical changes of the optical fiber itself, as well as physical changes in the environment around the optical fiber [10]. The measurement of the backscattered Rayleigh band can be implemented in distributed pressure measurements [11], magnetic fields detec-

Autor korespondujący:

Iyad S. M. Shatarah, iyad.shatarah@p.lodz.pl

Artykuł recenzowany

nadesłany 28.06.2023 r., przyjęty do druku 21.07.2023 r.



Zezwala się na korzystanie z artykułu na warunkach licencji Creative Commons Uznanie autorstwa 3.0

tion [12] or chemicals detection [13]. One may obtain temperature measurements alongside strain measurements along the optical fiber by measuring the backscattered Brillouin band [14]. However, the acquirement of only the temperature profile along the optical fiber by the measurement of the backscattered Raman anti-Stokes band is preferable, thus it is commonly used in distributed temperature sensing (DTS) systems [15]. DOFS systems are also used in the power cable monitoring [4], structure health monitoring [16], hydrology [17] and several other applications [18]. The DOFS systems measurements are performed in the optical time domain reflectometry (OTDR) [4], or in the optical frequency domain reflectometry (OFDR) [19].

The behavior of acoustic waves in optical fibers can be influenced by their construction and refractive index profiles, which can lead to variations in the Brillouin scattering parameters. To examine the behavior of acoustic waves and acousto-optic interactions in a limited geometry, it might also be helpful to compare the Brillouin gain spectra in various optical fibers types [20]. In this paper, two optical fibers are investigated in order to verify the impact of the optical fiber type on the quality of the obtained results of a DOFS system based on the measurement of the Brillouin backscattered band in the time domain. The first one is a standard optical fiber used in Fiber To The Home (FTTH) network, while the second is used in a long-haul networks due to lower attenuation. Obtained results can be handfull during the development of FTTH networks extended with temperature sensing abilities.

2. Backscattering in optical fibers

In optical fibers, light scattering is caused by the interaction between the light photons and the medium particles, and is enhanced by the variation of physical properties of the optical fiber and the surroundings. Light scattering is either elastic, where frequency of incident and the frequency of the scattered photons are equal, or inelastic, where the frequency of the scattered photons is shifted to lower (Stokes) or higher (anti-Stokes) frequencies [2]. Fig. 1 presents the light scattering spectrum. Light scatters in every direction. The main principle in the DOFS systems is the collecting of the backscattered light spectrum.

While the actual sensing mechanism in Brillouin-based DOFS systems relies on the measurement of the Brillouin frequency shift in order to calculate the strain and temperature variations, Raman-based DOFS systems measure the intensity of the Raman anti-Stokes band, which strongly depends on temperature [14]. In Raman-based DOFS systems, one may enhance the system's signal to noise ratio (SNR) by excluding the attenuation and fiber link losses, which is possible by registering the backscattered Rayleigh signals, then applying the demodulation algorithm to calculate the ratio between the Raman anti-Stokes signals and the Rayleigh signals [21].

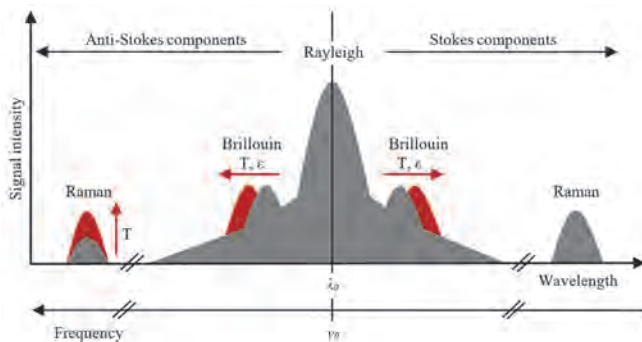


Fig. 1. The backscattered light spectrum
Rys. 1. Spektrum rozproszonego światła

Brillouin light scattering (BLS) is an interaction between photon and acoustic wave (phonon), where due to the annihilation of a photon of pump laser a Stokes photon and a phonon are created [16]. Hence, the frequency of the backscattered optical signal ν_{BS} is slightly lower than that of the incident light ν_p . The difference in frequency is related to the frequency of emitted phonons. The Brillouin frequency shift can be obtained by [22]:

$$|\nu_p - \nu_{BS}| = |\Delta\nu_B| = \frac{2n_{eff}}{\lambda_p} v_a, \quad (1)$$

where n_{eff} is the effective refractive index of optical fiber, v_a is the speed of the acoustic wave in the optical fiber, λ_p is the wavelength of incident light.

For silica-based optical fiber the value of the initial Brillouin frequency ν_{B0} is typically ranging from 9 to 11 GHz for 1550 nm incident wavelength. The number of Brillouin frequency peaks and their value and intensity depend on the type of optical fiber, where the refractive index profile has the most influence [23]. The refractive index depends on the temperature and strain, due to the thermo-optic and photo-elastic effects, respectively. Hence, the Brillouin frequency shift $\Delta\nu_B$ can be observed under the influence of temperature or strain changes along the length of the fiber [24]:

$$\Delta\nu_B = \nu_{B0} + C_T (T - T_0) + C_\epsilon (\epsilon - \epsilon_0), \quad (2)$$

where ν_{B0} is the initial Brillouin frequency, C_T and C_ϵ are the temperature and strain coefficients of optical fiber respectively, T and ϵ are the measured temperature and strain values respectively, T_0 and ϵ_0 are the reference temperature and strain values respectively. The temperature and strain coefficients are different for each optical fiber, resulting from the variety of acoustic velocities in different types of optical fibers [25]. Hence, a series of experiments must be held in order to determine the value of each coefficient for each optical fiber [26].

In order to distinguish the two measured values, it is necessary to use compensation methods, e.g. the implementation of two parallel fiber optic lines, one of which will not be susceptible to any stresses, or the implementation of optical fiber with different temperature and strain coefficients.

3. Measurement setup

In order to verify the impact of the optical fiber type and parameters, the measurement setup shown in Fig. 2 is built. The optical system consists of OZOptics DSTS unit, which is a Brillouin Optical Time Domain Reflectometer (BOTDR), operating at the wavelength of 1550 nm [27]. The wavelength of the laser used in this unit is 1550 nm. This unit allows the setting of the desired spatial resolution through the setting of the input laser pulse duration. The optical system is connected with PC unit for data acquisition and analysis. The BOTDR unit is connected through the optical fiber jumper to the prepared optical path, which includes two types of single-mode telecommunication optical fibers: sections 1, 2 and 3 are G.652.D optical fibers, while section 4 and 5 are G.654.C. Sections 2 and 4 are placed in the heat chamber in order to change their temperature. During the measurements, the temperature in the heat chamber was set to 20 °C, 40 °C or 70 °C. As mentioned above, both optical fibers are single-mode. However, the second optical fiber type, according

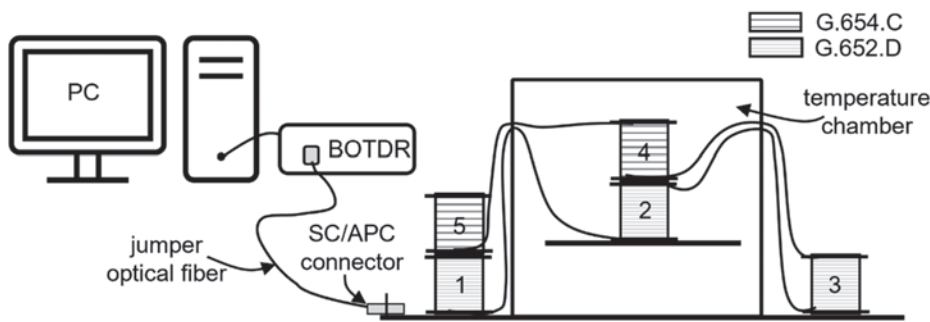


Fig. 2. The measurement setup
Rys. 2. Stanowisko pomiarowe

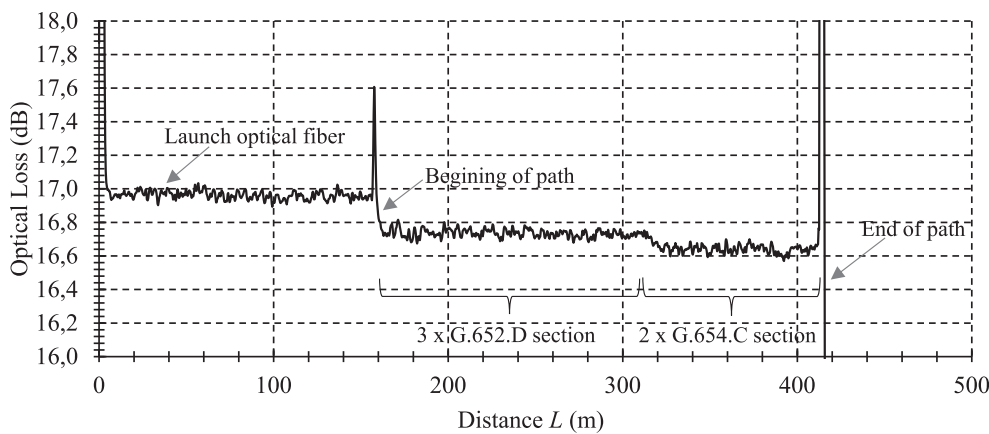


Fig. 3. OTDR reflectogram of tested optical fiber path with launch fiber, obtained by MAX730B
Rys. 3. Reflektogram OTDR badanego toru światłowodowego wraz z włóknem rozbiegowym, uzyskany z wykorzystaniem MAX730B

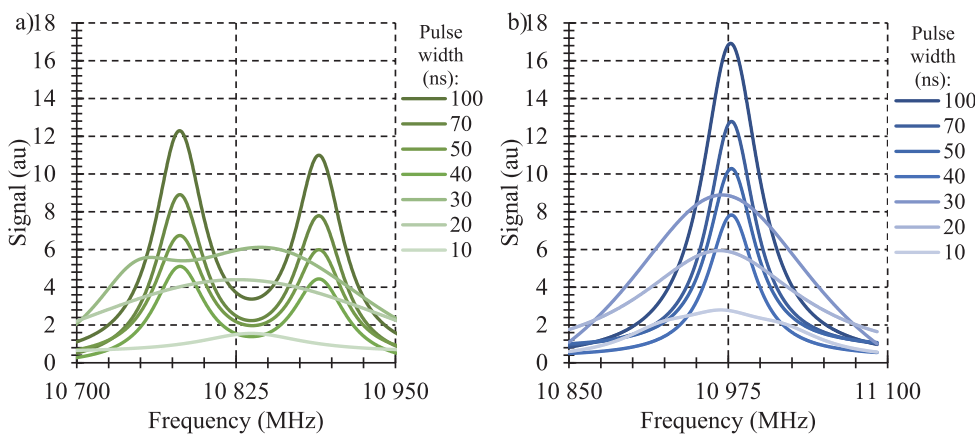


Fig. 4. Brillouin spectrum characteristics for both tested optical fibers: a) G.652.D and b) G.654.C
Rys. 4. Charakterystyki spektrum Brillouina dla obu badanych włókien światłowodowych: a) G.652.D i b) G.654.C

to ITU-T G.654.C standard is a cut-off shifted optical fiber which is used for high bandwidth long distance transmission.

Before the BOTDR tests, the optical fiber path is tested by standard reflectometer MaxTester730B by EXFO (wavelength 1550 nm, laser pulse 10 ns, averaging time 3 min) [28]. This reflectometer obtains the results through the measurement of the backscattered Rayleigh band. Based on the attenuation as a function of time, one may obtain the results of the optical losses along the optical path, as well as the actual length of each section of the tested optical path. The launch optical fiber at the first 160 m is used in order to stabilize the input light before entering the actual tested optical path. Then, the G.652.D sections optical fibers are visible, which are 160 m long. The G.654.C sections are about 100 m long.

4. Results

The first set of measurements involves the examination of the pulse width on the Brillouin frequency shift for both types of

optical fibers. The obtained results for the tested samples are presented in Fig. 4. As can be noticed for both optical fibers the frequency characteristic is initially wider, and with the increasing value of laser pulse width the signal is definitely narrower and stronger. Also, the frequency shift is different for each optical fiber type. Additionally, the G.652.D optical fiber has two Brillouin frequencies close to each other. In some optical fiber types, this results from the emergence of more than one acoustic wave, and as a result it is possible to monitor more than one Brillouin frequency shift [29]. Thus, implementing the wider input pulses allows obtaining results with better quality. The threshold value for both optical fibers is higher than 30 ns.

The second set of measurements involves the examination of temperature impact on the Brillouin frequency shift for the two types of optical fibers. Fig. 5 presents the Brillouin reflectogram for three exemplary different heat chamber temperature settings. The temperature tests are conducted based on the measurement setup presented in section 3. The measurements are conducted for 40 ns laser pulse width, where the dead zone

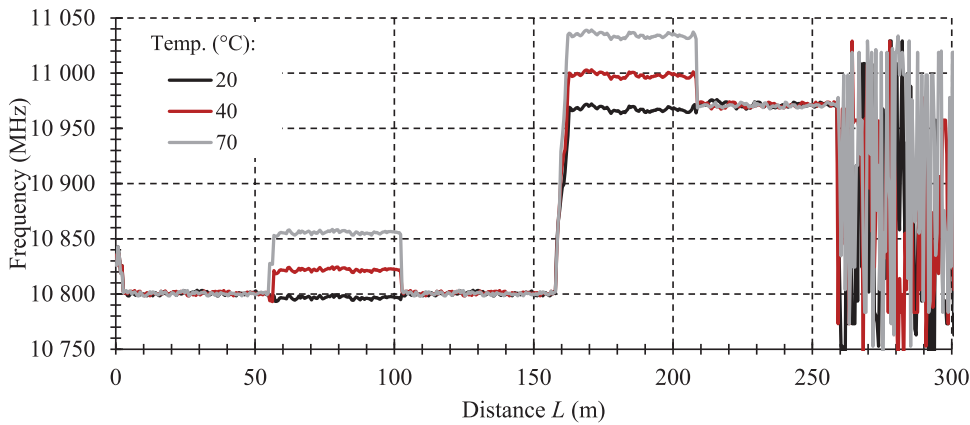


Fig. 5. BOTDR reflectogram of tested optical fiber path (without launch fiber)
 Rys. 5. Reflektogram BOTDR badanego toru światłowodowego (bez włókna rozbiegowego)

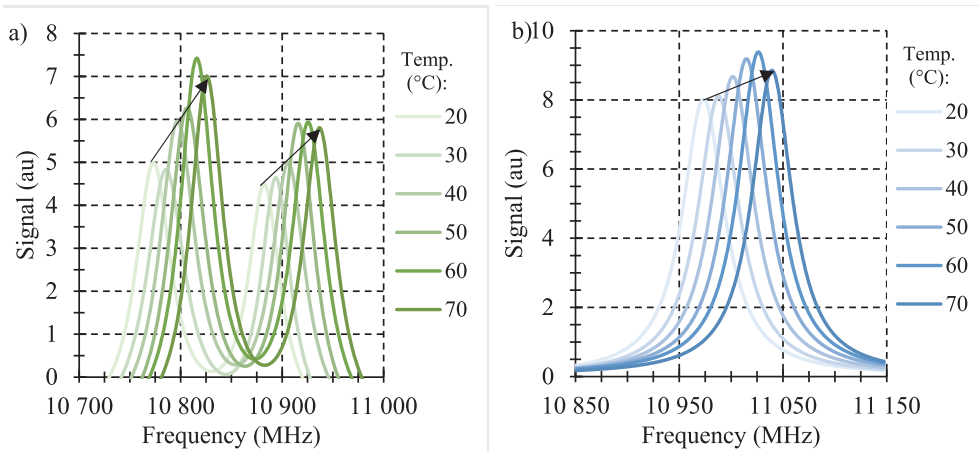


Fig. 6. Dependence of Brillouin frequency shift on temperature for a) G.652.D and b) G.654.C optical fibers
 Rys. 6. Zależność przesunięcia częstotliwości Brillouina od temperatury dla włókien światłowodowych a) G.652.D i b) G.654.C

is equal to about 4 m. This length may increase when the difference between Brillouin frequencies of two connected optical fibers is significant. Such case is visible at 160 m of path length. One may notice the temperature impact on the Brillouin frequency shift for the two sections of the optical fiber, which are placed in the heat chamber.

The shift of Brillouin characteristics for both optical fibers is shown in Fig. 6. The implementation of the 40 ns input laser pulses allows obtaining strong and narrow signal. As the temperature increases, the characteristics is drifting towards the higher frequencies. The width of the signal remains almost the same, whereas its intensity may slightly increase.

The full temperature tests were conducted in the range from $-20\text{ }^{\circ}\text{C}$ to $70\text{ }^{\circ}\text{C}$, where one cycle included the heating and cooling processes. The comparison of temperature coefficients are presented in Fig. 7. In the case of G.652.D optical fiber the both peaks were tracking. The frequency shift is highly linear ($R^2 > 0.997$) for both tested samples. The measured temperature coefficient equal to $1.4\text{ MHz}/^{\circ}\text{C}$ was definitely higher for G.654.C

optical fiber. For the standard optical fiber this parameter was equal to $1.12\text{ MHz}/^{\circ}\text{C}$ and $1.14\text{ MHz}/^{\circ}\text{C}$, respectively for the left and right peak.

5. Conclusions

The Brillouin specification for telecom optical fibers varies depending on its type. Moreover, the signal intensity response and its spectral width are related to the laser pulse width. For the tested fibers, the threshold value of this parameter was higher than 30 ns. Based on temperature cycle measurements, the G.654.C type optical fiber, according to ITU-T standard, has more potential to be used in sensor applications due to definitely higher temperature coefficient in comparison to sample of G.652.D optical fiber. The obtained value equals to $1.4\text{ MHz}/^{\circ}\text{C}$ for G.654.C fiber may be useful in realization of parallel channel for temperature compensation purposes during strain measurements.

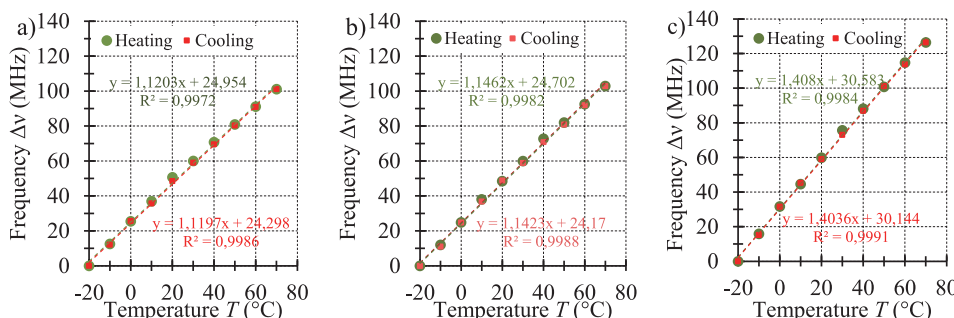


Fig. 7. The temperature cycles results for a) G.652.D fiber left peak and b) G.652.D fiber right peak, and c) G.654.C fiber
 Rys. 7. Wyniki krzywej temperatury badanych cykli nagrzewania i chłodzenia dla włókien światłowodowych a) G.652.D lewy szczyt b) G.652.D prawy szczyt, i c) G.654.C

Bibliography

1. Pendão C., Silva I., *Optical Fiber Sensors and Sensing Networks: Overview of the Main Principles and Applications*, "Sensors", Vol. 22, No. 19, 2022, 7554, DOI: 10.3390/s22197554.
2. Hartog A. H., *An Introduction to Distributed Optical Fibre Sensors*, "CRC Press", 1st edition, 2007. DOI: 10.1201/9781315119014.
3. Palmieri L., Schenato L., *Distributed Optical Fiber Sensing Based on Rayleigh Scattering*, "The Open Optics Journal", Vol. 7, 2013, 104–127, DOI: 10.2174/1874328501307010104.
4. Yilmaz G., Karlik S.E., *A distributed optical fiber sensor for temperature detection in power cables*, "Sensors and Actuators A" Physical", Vol. 125, No. 2, 2006, 148–155, DOI: 10.1016/j.sna.2005.06.024.
5. Seitz W.R., *Chemical Sensors Based on Fiber Optics*, "Analytical Chemistry", Vol. 56, No. 1, 1984, 16A–34A, DOI: 10.1021/ac00265a711.
6. Guzowski B., Łakomski M., *Temperature sensor based on periodically tapered optical fibers*, "Sensors", Vol. 21, No. 24, 2021, 8358, DOI: 10.3390/s21248358.
7. Gu H., Dong H., Zhang H., He J., Pan H., *Effects of Polymer Coatings on Temperature Sensitivity of Brillouin Frequency Shift Within Double-Coated Fibers*, "IEEE Sensors Journal" Vol. 13, No. 2, 2013, 864–869, DOI: 10.1109/JSEN.2012.2230438.
8. Juan H.D.J., Humbert G., Dong H., Zhang G., Hao J., Sun Q., *Review of Specialty Fiber Based Brillouin Optical Time Domain Analysis Technology*, "Photonics", Vol. 8 No. 10, 2021, 421, DOI: 10.3390/photonics8100421
9. Torre U., *Conveyor fire detection & condition monitoring using fibre optic distributed temperature sensing (DTS)* "Advanced Photonics Australia", 2017, available at: <https://apapl.com.au/wp-content/uploads/2022/10/Conveyor-Fire-Detection-and-Condition-Monitoring-using-DTS-Paper.pdf>
10. Thomas P.J., Hellevang J.O., *A fully distributed fibre optic sensor for relative humidity measurements*, "Sensors and Actuators B: Chemical", Vol. 247, 2017, 284–289, DOI:10.1016/j.snb.2017.02.027.
11. Rogers A.J., Shatalin S.V., Kanellopoulos S.E., *Distributed measurement of fluid pressure via optical-fibre backscatter polarimetry*, "Proc. SPIE 5855, 17th International Conference on Optical Fibre Sensors", Vol. 5855, 2005, 230–233, DOI: 10.1117/12.623804.
12. Ross J.N., *Measurement of magnetic field by polarisation optical time-domain reflectometry*, "Electronics Letters", Vol. 17, No. 17, 1981, 596–597, DOI: 10.1049/el:19810419.
13. Cordero S.R., Ruiz D., Huang W., Cohen L.G., Lieberman R.A., *Intrinsic chemical sensor fibers for extended-length chlorine detection*, "Proc. SPIE 5589, Fiber Optic Sensor Technology and Applications III", 2004, DOI: 10.1117/12.605489.
14. Shimizu K., Horiguchi T., Koyamada Y., *Measurement of distributed strain and temperature in a branched optical fiber network by use of Brillouin optical time-domain reflectometry*, "Optics Letters", Vol. 20, No. 5, 1995, 507–509, DOI: 10.1364/OL.20.000507.
15. Suárez F., Dozier J., Selker J., Hausner M.B., Tyler S.W., *Heat Transfer in the Environment: Development and Use of Fiber-Optic Distributed Temperature Sensing*, "Developments in Heat Transfer", InTech, 2011, DOI: 10.5772/19474.
16. Sienko R., Zych M., Bednarski Ł., Howiacki T., *Strain and crack analysis within concrete members using distributed fibre optic sensors*, "Structural Health Monitoring", Vol. 18, No. 5–6, 1510–1526, DOI: 10.1177/1475921718804466.
17. Selker J.S., Thévenaz L., Huwald H., Mallet A., Luxemburg W., van de Giesen N., Stejskal M., Zeman J., Westhoff M., Parlange M.B., *Distributed fiber-optic temperature sensing for hydrologic systems*, "Water Resources Research", Vol. 42, No. 12, W12202, 2006, DOI: 10.1029/2006WR005326.
18. Ukil A., Braendle H., Krippner P., *Distributed temperature sensing: Review of technology and applications*, "IEEE Sensors Journal", Vol. 12, No. 5, 2011, 885–892, DOI: 10.1109/JSEN.2011.2162060.
19. Farahani M.A., Gogolla T., *Spontaneous Raman Scattering in Optical Fibers with Modulated Probe Light for Distributed Temperature Raman Remote Sensing*, "Journal of Lightwave Technology", Vol. 17, No. 8, 1999, 1379–1391, DOI: 10.1109/50.779159.
20. Yeniay A., Delavaux J.M., Toulouse J., *Spontaneous and stimulated Brillouin scattering gain spectra in optical fibers*, "Journal Of Lightwave Technology", Vol. 20, No. 8, 1425, 2002, DOI: 10.1109/JLT.2002.800291.
21. Ly J., et al., *Performance Improvement of Raman Distributed Temperature System by Using Noise Suppression*, "PHOTONIC SENSORS", Vol. 8, No. 2, 103–113, 2018, DOI: 10.1007/s13320-017-0474-5.
22. Lu P., Lalam N., Badar M., Chorpening B.T., Buric M.P., Ohodnicki P.R., *Distributed optical fiber sensing: Review and perspective*, "Applied Physics Reviews", Vol. 6, No. 4, 2019, 041302, DOI: 10.1063/1.5113955.
23. Ippen E., Stolen R., *Stimulated Brillouin scattering in optical fibers*, "Appl. Phys. Lett." Vol. 21, 1972, 539–541, DOI: 10.1063/1.1654249.
24. Lakomski M., Tosik G., *Brillouin backscattering analysis in recent generation of telecom optical fibers*, "Optica Applicata", Vol. 52, No. 3, 2022, 405–416, DOI: 10.37190/oa220307.
25. Horiguchi T., Shimizu K., Kurashima T., Tateda M., Koyamada Y., *Development of a distributed sensing technique using Brillouin scattering*, "Journal of Lightwave Technology", Vol. 13, No. 7, 1995, 1296–1302, DOI: 10.1109/50.400684.
26. Ismail A., Qurratu Aini binti Siat @ Sirat, Azman bin Kasim, Hisham bin Mohamad, *Strain and temperature calibration of Brillouin Optical Time Domain Analysis (BOTDA) sensing system*, "IOP Conference Series: Materials Science and Engineering", Vol. 527, 2019, 012028, DOI: 10.1088/1757-899X/527/1/012028.
27. OZOptics BOTDR DSTS module datasheet. Available at: https://www.ozoptics.com/ALLNEW_PDF/DTS0138.pdf.
28. EXFO MaxTester730B OTDR reflectometer datasheet. Available at: <https://www.exfo.com/umbraco/surface/file/download/?ni=11066&cn=en-US&pi=5644>.
29. Zou W., He Z., Hotate K., *Complete discrimination of strain and temperature using Brillouin frequency shift and birefringence in a polarization-maintaining fiber*, "Optics Express", Vol. 17, 2009, 1248–1255, DOI: 10.1364/OE.17.001248.

Wpływ typu światłowodu na pomiar temperatury w systemach rozłożonych czujników światłowodowych

Streszczenie: W artykule przedstawiono możliwości wykorzystania rozłożonych czujników światłowodowych do uzyskania rozkładu temperatury wzdłuż toru optycznego wykonanego z telekomunikacyjnego włókna światłowodowego. Obserwowany jest również wpływ rodzaju włókna światłowodowego na pomiary temperatury. Przetestowano dwa rodzaje włókien światłowodowych: standardowe G.652.D oraz o niskiej stratności G.654.C. Systemy DOFS do pomiarów temperatury wykorzystują zjawisko wstecznych rozpraszania Ramana lub Brillouina. W przypadku systemów bazujących na zjawisku Brillouina, właściwości spektralne zależą od rodzaju włókna optycznego oraz jego parametrów. Przesunięcie częstotliwości Brillouina zależy od temperatury wokół włókna oraz nałożonego na włókno naprężenia. Przedstawione wyniki pokazują, że współczynnik temperaturowy może również różnić się w zależności od rodzaju włókna optycznego. Dla standardowego włókna światłowodowego G.652.D, współczynnik temperaturowy wynosi 1,12 MHz/°C lub 1,14 MHz/°C w zależności od śledzonych szczytów, podczas gdy dla włókna o niskiej stratności G.654.C wynosi 1,4 MHz/°C.

Słowa kluczowe: światłowód, DOFS, OTDR, rozpraszanie Brillouina

Mateusz Łakomski, PhD, Eng.

mateusz.lakomski@p.lodz.pl
ORCID: 0000-0002-1341-0215



He received the Ph.D. degree in Electronics Engineering from Lodz University of Technology, Poland. Since 2015, he has been a Research Assistant at the LUT working in Laboratory of Optical Fiber Technique. From 2018 to 2021, he was a Scientific and Technical Specialist at LUT specialized in optical fiber strain monitoring. From 2023 he works as assistant professor position at LUT. His research interest includes the development of optical fiber application area, especially sensors and improvement of optical fiber coupling loss.

Iyad S.M. Shatarah, MSc, Eng.

iyad.shatarah@p.lodz.pl
ORCID: 0000-0002-4297-1986



He received the M.Sc. degree in Electronics and Telecommunications Engineering from Lodz University of Technology, Poland in 2014. Currently, he is pursuing the Ph.D. degree in Electronics Engineering at Lodz University of Technology, Poland. He started working at the Institute of Electronics at Lodz University of Technology since 2019 as a Senior Technical Referent, and as an Assistant since 2021. His scientific interests are optoelectronics, fiber optic sensors and thermography.

Mateusz Plona, BSc, Eng.

222228@edu.p.lodz.pl
ORCID: 0009-0007-4745-0278



He was born in Mragowo, Poland in 1998. He received a B.E degree in Electronics and Telecommunications Engineering from Lodz University of Technology, Lodz, Poland in 2021. He is currently pursuing a M.Sc. degree in Electronic and Telecommunication at Lodz University of Technology, Lodz, Poland. Since 2021, he has been a designer of telecommunications lines for PRO-MATT. He is keen on fiber optics systems, especially sensors and networks. He has been the recipient of scholarships awarded for academic performance, including the Rector's scholarship at Lodz University of Technology in 2021.

Bartłomiej Guzowski, PhD, Eng.

bartlomiej.guzowski@p.lodz.pl
ORCID: 0000-0002-6090-1359



He received a Ph.D. degree in 2014 from Lodz University of Technology, Poland. He works as assistant professor in Department of Semiconductor and Optoelectronics Devices. His scientific interests are optoelectronics, fiber optic sensors and energy harvesting. He is the author of numerous publications in his field of interest.